Growth and optical properties of $(Na_{0.5}Bi_{0.5})(Mo_{1-x}W_x)O_4$ (x = 0.25) single crystal: A potential candidate for optoelectronic devices

I. Guler[a], M. Isik[b] , N. Gasanly[c]

[a]*Physics, Inter-Curricular Courses Department, Çankaya University, 06530 Ankara, Turkey*
[b]*Department of Electrical and Electronics Engineering, Atilim University, 06836 Ankara, Turkey*
[c]*Department of Physics, Middle East Technical University, 06800 Ankara, Turkey*

Abstract

Double tungstates (DT) and double molybdates (DM) have significant importance because of their optoelectronic applications. Regarding the importance of DT and DM, we investigated experimentally structural and optical properties of $(Na_{0.5}Bi_{0.5})(Mo_{1-x}W_x)O_4$ (x = 0.25) crystal that belongs to the NaBi-DT and DM crystals group. Czochralski method was used to grow the single crystals. The structure of the crystal was identified using X-ray diffraction (XRD) measurements. Two sharp peaks associated with tetragonal crystal structure appeared in the pattern. Vibrational modes of the studied crystal were obtained from the Raman experiments. By the help of the Fourier transform infrared spectrophotometer (FTIR) measurements, infrared transmittance spectrum of the studied compound was recorded. Band gap energy wase found around 3.04 eV using two methods, Tauc and derivative analysis, based on transmission spectrum. Based on the analysis of absorption coefficient, Urbach energy was obtained as 0.22 eV. The revealed structural and optical properties of the crystal indicated that the material may be a candidate for optoelectronic devices in which $NaBi(MoO_4)_2$ and $NaBi(WO_4)_2$ materials are utilized.

Keywords: Double tungstates; Double molybdates; XRD; Optical properties

E-mail address: mehmet.isik@atilim.edu.tr

Published by OPTICAL AND QUANTUM ELECTRONICS
https://doi.org/10.1007/s11082-023-05549-3

1. Introduction:

Double tungstates and molybdates have significant importance because of their use as laser media. They have chemical formula of $XT(YO_4)_2$ (*X*: monovalent cation, *T*: trivalent one, *Y*: Mo^{6+} or W^{6+}). Among these groups, bismuth based compounds draw attention as visible light induced photo catalyst thanks to its light absorption characteristics [1–4]. Double sodium–bismuth molybdate $NaBi(MoO_4)_2$ has exciting characteristics like high luminous efficiency and density, fast response time, good anti-irradiation. These characteristics make the compound potential in high energy, luminescence and safety-checking device applications [5]. It presents well luminescence, photocatalytic, photo elastic, acoustic, and sensing characteristics [6–12]. The band gap energy of $NaBi(MoO_4)_2$ compound was reported generally in between 2.9 and 3.1 eV [11,13]. Double sodium–bismuth tungstate $NaBi(WO_4)_2$ enters the field of interest of scientists for ultra-high energy radiation detection and charged particles in the TeV region [14,15]. The physical properties and crystalline structure of crystals of $NaBi(WO_4)_2$were investigated in [16, 17]. Waskowska et al. [18] studied electronic and optical characteristics of $NaBi(WO_4)_2$ and using the generalized gradient approximation, its indirect band gap was calculated as 3.2 eV. Kato et al. [13] found the direct band gap of the material as 3.5 eV.

In the $NaBi(MoO_4)_2$ compound, as a result of the substitution of Mo element with W, $(Na_{0.5}Bi_{0.5})(Mo_{1-x}W_x)O_4$ compounds are formed. The structural and optical features of each compound formed by changing the composition in the range of $0 \leq x \leq 1$ may tune and this tuning behavior provides various benefits in technological applications. Unfortunately, the studies on $(Na_{0.5}Bi_{0.5})(Mo_{1-x}W_x)O_4$ compounds in the literature are almost non-existent. A recent study examined the microwave dielectric characteristics of the compositions of x = 0.0, 0.5 and 1.0 [19]. As a result of revealed characteristics, author stated that $(Na_{0.5}Bi_{0.5})(Mo_{1-x}W_x)O_4$ ceramics have remarkable potential to be used in low temperature co-fired ceramic area. Regarding the importance of the NaBi-double tungstate and molybdate crystals mentioned above and advantages of tuning characteristics of the mixed compounds, we investigated experimentally structural and optical properties of $(Na_{0.5}Bi_{0.5})(Mo_{1-x}W_x)O_4$ (x = 0.25) crystal. X-ray diffraction, Raman and infrared spectroscopy, transmission measurements were performed as characterization techniques.

2. Experimental

Czochralski method was used to grow $(Na_{0.5}Bi_{0.5})(Mo_{0.75}W_{0.25})O_4$ crystals. Ratio of the starting compounds in the growth process was $1Bi_2O_3$: $3MoO_3$:$1WO_3$:$1Na_2CO_3$. The starting

compounds were mixed and resulting mixture was pressed to obtain pellets. The pellets were heated around 800 ^{o}C for 24 hour to obtain single phase. During growing, 2 mm/h pulling rate and 15 rpm rotation rate was performed. After crystal growth completed, the crystal polished and cut in size of 13 × 6 × 2 mm^3. The single crystal that was grown and examined within the scope of this study is shown in Figure 1. For X-ray diffraction (XRD) experiments, Rigaku miniflex model diffractometer that emits CuK_{α} radiation at wavelength of 0.154049 nm from 10 to 80° with a speed of 0.02°/s was used. Raman scattering measurements were achieved by 532 nm Nd:YAG laser source by Horiba Jobin Yvon iHR550 imaging spectrometer. The transmission measurements were accomplished in the 350-700 nm range by Jenway 6400 model spectrophotometer. Infrared transmittance spectrum was recorded in the 2400-3200 cm^{-1} range by Nicolet 6700 FTIR spectrometer having resolution of 2 cm^{-1}.

3. Results and discussion

Figure 1 represents XRD pattern of the $(Na_{0.5}Bi_{0.5})(Mo_{0.75}W_{0.25})O_4$ crystal in the range of 10-80°. Two peaks centered at 35.20° and 72.40° were observed in the diffraction pattern. According to JCPDS Card, the observed intense peaks were associated with the planes of (200) and (400) associated with tetragonal scheelite structure. This result is consistent with previously published reports of $NaBi(MoO_4)_2$ and $NaBi(WO_4)_2$ [18-21]. Moreover, XRD analysis of the $(Na_{0.5}Bi_{0.5})(Mo_{1-x}W_x)O_4$ ($x = 0$, 0.5 and 1.0) were done [19] and it was established that the corresponding compounds crystallize in tetragonal scheelite structure which is consistent with our result revealed for x = 0.25.

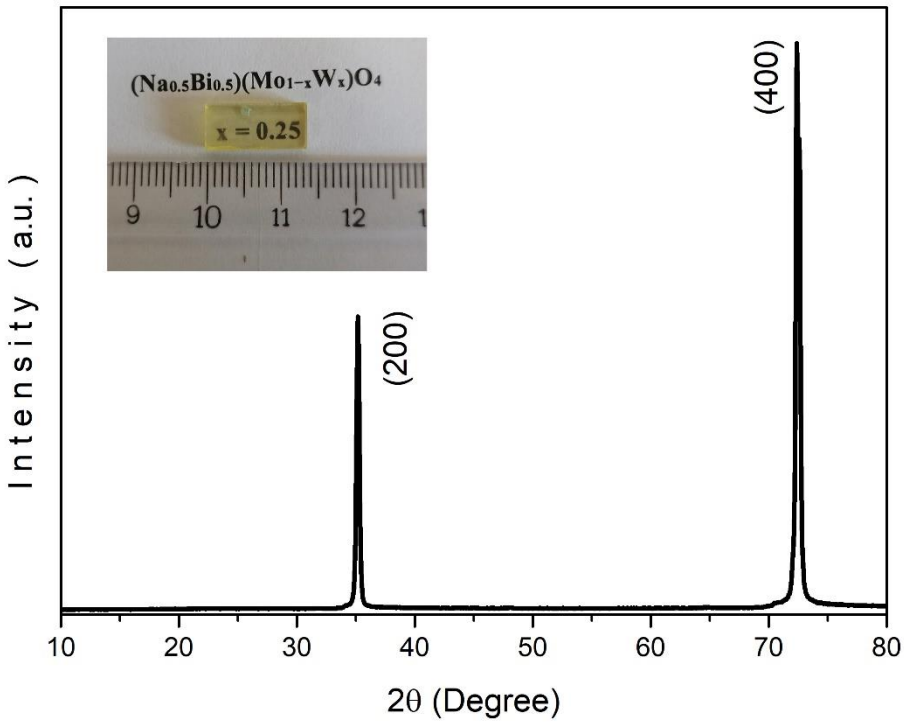

Figure 1. XRD pattern of $(Na_{0.5}Bi_{0.5})(Mo_{0.75}W_{0.25})O_4$ crystal. Inset indicates the image of the grown crystal.

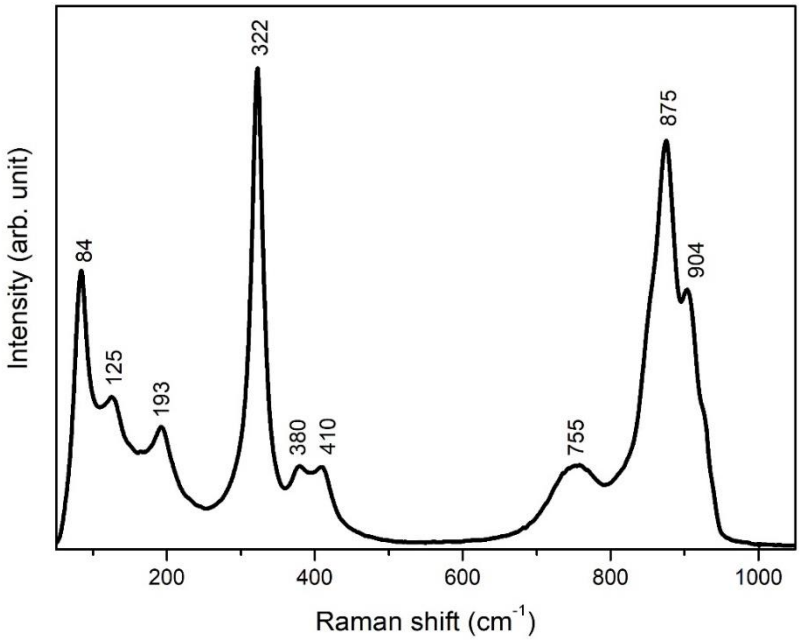

Figure 2. Raman spectrum of $(Na_{0.5}Bi_{0.5})(Mo_{0.75}W_{0.25})O_4$ crystal.

Figure 2 represents the Raman spectrum giving information about vibrational, electronic states, structural and phonon properties of the crystal. Nine Raman peaks centered at 84, 125, 193, 322, 380, 410, 755, 875 and 904 cm^{-1} were observed. The peaks have good agreement with results reported by Sal et al. [22]. Sal et al. reported the Raman peaks noted at 192, 321, 376, 414, 770 and 875 cm^{-1} for opal nanocomposites of $NaBi(MoO_4)_2$. The bands at near 84 and 125 cm^{-1} are related to B_g symmetry and E_g, respectively. These bands may be associated with $T'(MoO_4^{2-})$ and $T'(Bi^{3+})$ phonons. The band centered at 193 cm^{-1} may be related to the coupled $T'(Na)$ and $L(MoO_4^{2-})$ modes. One of the strong vibrational modes near 875 cm^{-1} was assigned to the symmetrical vibrational mode of MoO_4^{2-} tetrahedra, and the weak peak around 755 cm^{-1} was assigned to the anti-symmetric Mo-O stretching mode. The mode around 322 cm^{-1} was related to the symmetric Mo-O bending vibration. The peak around 380 cm^{-1} comes from asymmetric bending of MoO_4^{2-} [23]. The vibrational band around 410 cm^{-1} exists due to the asymmetric bending of MoO_4^{2-} tetrahedra. This information was presented in Table 1 that also gives comparison of the Raman modes frequencies of $(Na_{0.5}Bi_{0.5})(Mo_{0.75}W_{0.25})O_4$, $NaBi(MoO_4)_2$ and $NaBi(WO_4)_2$ from literature [21-26].

Table 1. Raman frequencies of $NaBi(MoO_4)_2$, $(Na_{0.5}Bi_{0.5})(Mo_{0.75}W_{0.25})O_4$ and $NaBi(WO_4)_2$

$NaBi(MoO_4)_2$			$Na_{0.5}Bi_{0.5}(Mo_{0.75}W_{0.25})O_4$	$NaBi(WO_4)_2$		
[22]	[24]	[25]	Our work	[21]	[26]	[24]
		48				
				67	69	72
	89	90	84			
				113	114	104
	130	130	125			
192	195	192	193	195	198	198
321	323	319	322	329	329	331
376	376	375	380	388	386	398
414		408	410	415	416	
			755		750	
770	777	768		764	766	766
875	877	876	875	878	875	
	914	911	904	910	910	910
	930	930		928	925	

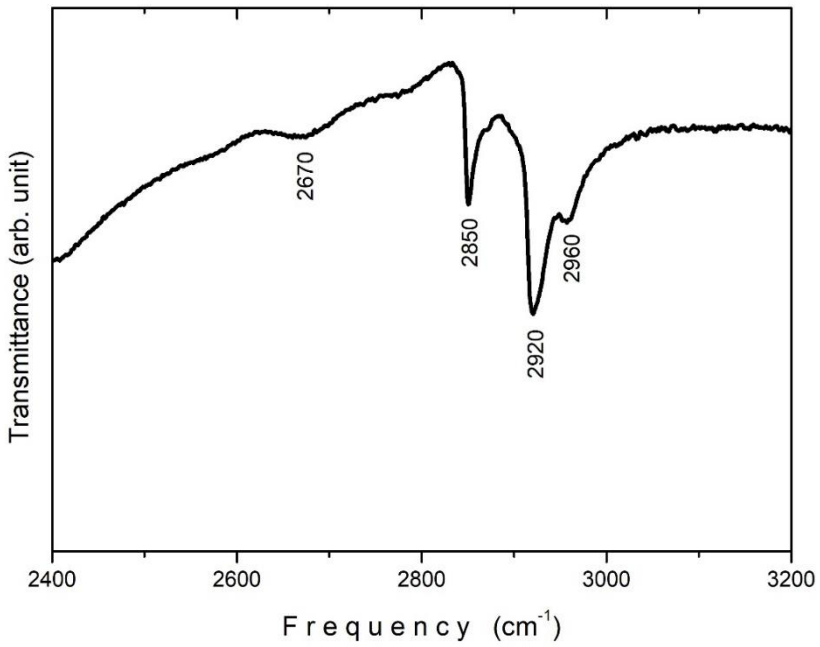

Figure 3. FTIR transmittance spectrum of $(Na_{0.5}Bi_{0.5})(Mo_{0.75}W_{0.25})O_4$ crystal.

FTIR measurements were performed to get information about the infrared transmittance of the crystal. The FTIR transmittance spectrum of the $(Na_{0.5}Bi_{0.5})(Mo_{0.75}W_{0.25})O_4$ crystal were indicated in Figure 3 in the frequency range of 2400-3200 cm^{-1}. The absorptions at 2850 cm^{-1} associate with symmetric C-H stretching [27-29]. The band at 2920 cm^{-1} and 2960 cm^{-1} are due to C-H asymmetric stretching vibration mode [30]. The peak around 2670 cm^{-1} represents the asymmetric C-H stretching vibrations [31]. However, in many studies, the observed peaks were associated with C-H vibrations. Juchem et al. [32] observed absorption bands for fuchsite quartzite stones and emerald stones at 2850 and 2920 cm^{-1}, with a shoulder at ± 2953 cm^{-1}. Only for quartzite stone, absorption peak was observed at 2670 cm^{-1}. The peaks at 2850, 2920 and 2953 cm^{-1} that resembling data shown for universal oil by Johnson et al. (1999) and by Kiefert et al. [33, 34]. As a result, fuchsite quartzite stones and emerald stones were like paraffin oil and wax, Joban oil and HXTAL resin. Based on these works, we may conclude as $(Na_{0.5}Bi_{0.5})(Mo_{0.75}W_{0.25})O_4$ crystal shows absorbance like quartzite stones.

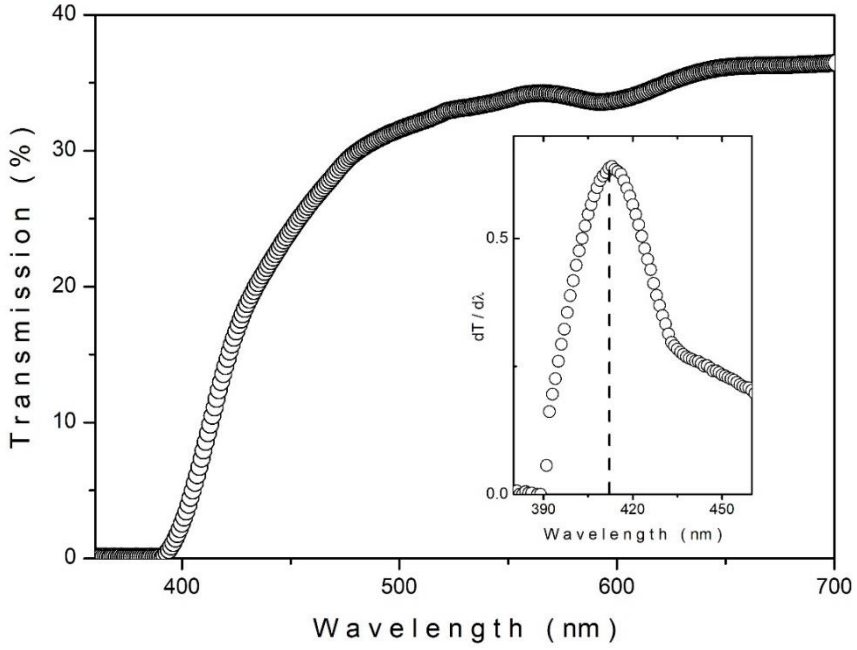

Figure 4. Transmission spectrum of $(Na_{0.5}Bi_{0.5})(Mo_{0.75}W_{0.25})O_4$ crystal. Inset: $dT/d\lambda$ vs. λ plot.

Transmission spectrum given in Figure 4 in the range of 360-700 nm was reported to get information about optical properties of the $(Na_{0.5}Bi_{0.5})(Mo_{0.75}W_{0.25})O_4$ crystal. In order to find the band gap energy (E_g), Tauc [35] and derivative spectroscopy analyses were used. In the derivative spectroscopy technique, the derivative of the transmission spectrum is taken with respect to the wavelength and $dT/d\lambda$ vs. λ graph shown in the inset of Figure 4 is drawn. The peak maximum position of the peak observed in this plot corresponds to band gap energy. The graph drawn showed one peak around 413 nm corresponding to energy of 3.01 eV. When we compare the band gap of the studied crystal of $(Na_{0.5}Bi_{0.5})(Mo_{1-x}W_x)O_4$ for $x = 0.25$ with those of $x = 0$ (~2.90 eV) and $x = 1$ (~3.50 eV), the revealed band gap is within the band gaps of these compounds.

Tauc equation is given below where hv is photon energy, α is the absorption coefficient, A is a parameter related to transition probability and p is 2 for indirect transitions or 1/2 for direct transitions.

$$(\alpha h\nu) = A(h\nu - E_g)^p \quad (1)$$

The absorption coefficient was calculated from transmittance (T) and thickness (d) of the sample by $\alpha = (1/d) \ln (1/T)$. Using equation (1), the band gap energy can be found by plotting

$(\alpha hv)^{1/p}$ vs. hv graph. Figure 5 indicates the $(\alpha hv)^2$ vs. hv plot which present linear dependency around the strong absorption range. The direct band gap of the crystal was found from the linear fit of the dependency as 3.04 eV that is well-consistent with energy revealed from derivative analysis.

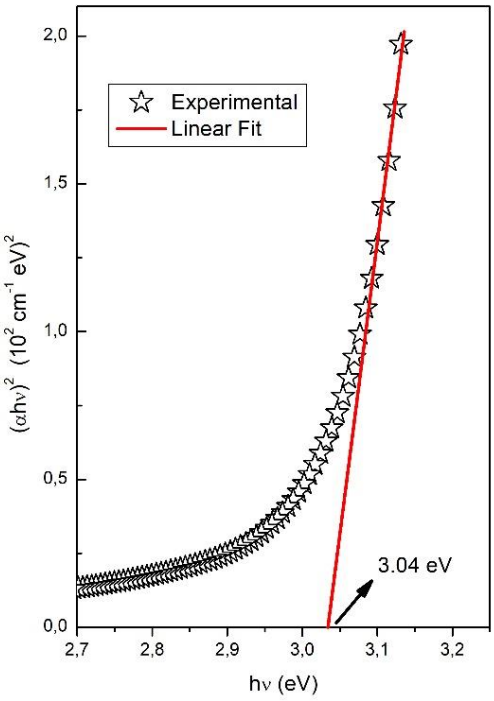

Figure 5. $(\alpha hv)^2$ vs. hv plot of $(Na_{0.5}Bi_{0.5})(Mo_{0.75}W_{0.25})O_4$ crystal.

Urbach energy (E_u) of the compound was obtained from the analysis of the dependency of absorption coefficient on photon energy represented in Fig. 6. The relation between α and E_u is given as in the following equation below [36]

$$\alpha(hv) = \alpha_0 \exp\left(hv/E_u\right) . \quad (2)$$

When this equation is rearranged, ln(α) vs. hv plot presents a linear dependence having slope of $1/E_u$. Inset of Figure 6 represents the mentioned plot and applied linear fitted. Urbach energy was calculated from the slope of the fitted line as 0.22 eV.

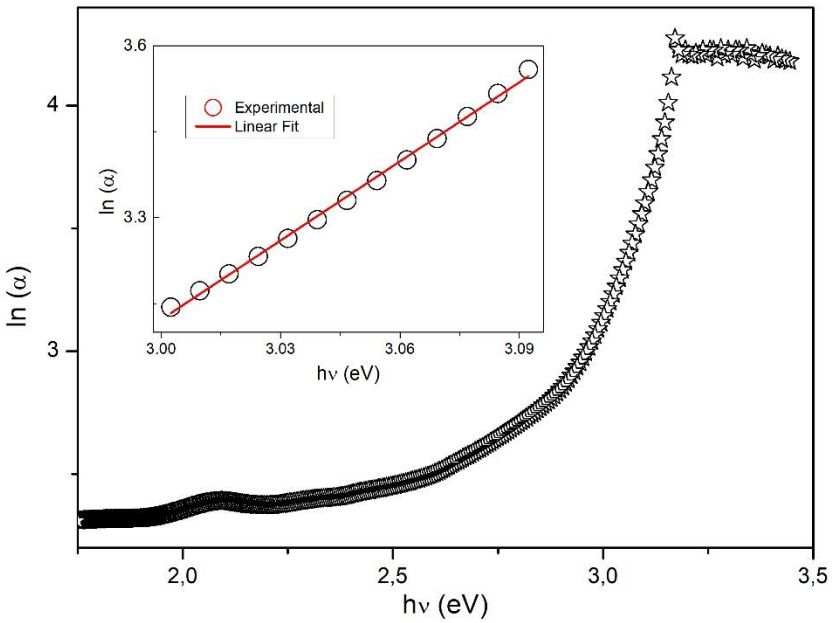

Fig. 6. The dependency of absorption coefficient to photon energy. Inset shows the ln(α) vs. $h\nu$ plot for Urbach energy analysis.

4. Conclusion

In this study, the structural and optical properties of $(Na_{0.5}Bi_{0.5})(Mo_{1-x}W_x)O_4$ (x = 0.25) crystal grown by Czochralski method were presented. Two peaks centered at 35.20° and 72.40° were observed in the XRD pattern. These peaks were associated with parallel planes of tetragonal scheelite structure. Nine vibrational modes of the crystal were revealed from Raman measurements. From the infrared transmittance spectrum, the peaks observed at 2670 cm^{-1}, 2850 cm^{-1}, 2920 cm^{-1} and 2953 cm^{-1} of the crystal show that it has transmittance like quartzite stones acting like paraffin oil and wax, Joban oil and HXTAL resin. Room temperature transmission experiments were performed, and the band gap energy of the crystal was found as 3.04 eV and 3.01 eV using Tauc and derivative analysis method, respectively. Urbach energy was also determined from the analysis as 0.22 eV. Taking into account the 3.04 eV direct band gap and usage areas of $NaBi(MoO_4)_2$ and $NaBi(MoO_4)_2$, the grown of the $Na_{0.5}Bi_{0.5}(Mo_{0.75}W_{0.25})O_4$ compound may be a potential candidate especially in optoelectronic devices. A bandgap energy of 3.04 eV suggests that the material might be suitable for photovoltaic applications that involve capturing high-energy photons, such as ultraviolet or blue light. The relatively large bandgap energy makes the material a candidate for UV

photodetectors, as it can absorb and detect UV light effectively. Moreover, the relatively wide bandgap energy suggests that the material could be suitable for photocatalytic reactions driven by higher-energy UV photons. UV photocatalysis is used in applications like water purification, air cleaning, and degradation of organic pollutants.

Declarations:

Ethical Approval

Not applicable

Competing interests

The authors have no competing interests to declare that are relevant to the content of this article.

Authors' contributions

I.G., M.I. and N. G. wrote the main manuscript text

I.G. and M.I. did formal analysis and investigation

N.G. reviewed and edited manuscript text

I.G. and M.I. prepared all figures and table

Funding

The authors declare that no funds, grants, or other support were received during the preparation of this manuscript.

Availability of data and materials

The data that support the findings of this study are available from the corresponding authors upon reasonable request.

References

[1] J.L. Zhang, L.S. Zhang, N. Yu, K.B. Xu, S.J. Li, H.L. Wang, J.S. Liu, Flower-like Bi_2S_3/Bi_2MoO_6 heterojunction superstructures with enhanced visible-light-driven photocatalytic activity, RSC Adv. 5 (2015) 75081–75088. https://doi.org/10.1039/C5RA13148K.

[2] J.S. Cai, J.Y. Huang, Y.K. Lai, $BiMoO_6$ nanosheet/TiO_2 nanotube array heterostructure with enhanced UV and visible-light photocatalytic activity, J. Mater. Chem. A 5 (2017) 16412–16421. https://doi.org/10.1039/C7TA02077E.

[3] J. Liu, R. Wei, J. Hu, L. Li, J. Li, Novel $Bi_2O_3/NaBi(MoO_4)_2$ heterojunction with enhanced photocatalytic activity under visible light irradiation, J. Alloy. Compd. 580 (2013) 475–480. https://doi.org/10.1016/j.jallcom.2013.06.154.

[4] M. Zhang, Y. Qi, Z. Zhang, AgBr/BiOBr nano-heterostructure-decorated polyacrylonitrile nanofibers: a recyclable high-performance photocatalyst for dye degradation under visible-light irradiation, Polymers 11 (2019) 1718 1-12. https://doi.org/10.3390/polym11101718.

[5] Zb. Mazurak, G. Blasse, J. Liebertz, The luminescence of the scheelite $NaBi(MoO_4)_2$, J. Solid State Chem. 68 (1987) 181-184. https://doi.org/10.1016/0022-4596(87)90301-X.

[6] M. Xu, Z. Lin, Y. Hong, Z. Chen, P. Fu, D. Tang, Preparation and hydrogen sulfide gas-sensing performances of RuO_2/NaBi-$(MoO_4)_2$ nanoplates. J. Alloy. Compd. 688 (2016) 504−509. http://dx.doi.org/10.1016/j.jallcom.2016.07.007.

[7] L. Liu, H. Wang, X. Zhang, Z. Lin, Synthesis of novel RuO_2/$NaBi(MoO_4)_2$ nano-sheets composite and its gas sensing performances towards ethanol, Sens. Actuat. B 237 (2016) 275−283. https://doi.org/10.1016/j.snb.2016.06.095.

[8] O. Krupych, M. Kushnirevych, O. Mys,R. Vlokh, Photoelastic properties of $NaBi(MoO_4)_2$ crystals, Appl. Opt. 54 (2015) 5016−5023. https://doi.org/10.1364/AO.54.005016.

[9] L. Khusravbekov, A. Kholov, E.V. Charnaya, Acoustic investigation of $NaBi(MoO_4)_2$ and $NaBi(WO_4)_2$ crystals at high temperatures. Bull. Russ. Acad. Sci.: Phys. 79 (2015) 1306−1309. https://doi.org/ 10.3103/S1062873815100135.

[10] Pushpendra, R.K. Kunchala, R. Kalia, B.S. Naidu, Upconversion luminescence properties of $NaBi(MoO_4)_2$:Ln^{3+}, Yb^{3+} (Ln = Er, Ho) nanomaterials synthesized at room temperature. Ceram. Int. 46 (2020) 18614–18622. https://doi.org/10.1016/j.ceramint.2020.04.173.

[11] Y.J. Li, T.P. Can, Z.M. Mei, X.P. Li, D.W. Sun, Separating type I heterojunction of $NaBi(MoO_4)_2$/Bi_2MoO_6 by TiO_2 nanofibers for enhanced visible-photocatalysis, Chem. Phys. 533 (2020) 110696. https://doi.org/10.1016/j.chemphys.2020.110696.

[12] Pushpendra, R.K. Kunchala, S.N. Achary, A.K. Tyagi, B.S. Naidu, Rapid, room temperature synthesis of Eu^{3+} doped $NaBi(MoO_4)_2$ nanomaterials: structural optical, and photoluminescence properties, Cryst. Growth Des. 19 (2019) 3379–3388. https://doi.org/10.1021/acs.cgd.9b00267.

[13] H. Kato, N. Matsudo, A. Kudo, Photophysical and photocatalytic properties of molybdates and tungstates with a scheelite structure, Chem. Lett. 33 (2004) 1216-1217. https://doi.org/10.1246/cl.2004.1216.

[14] G.I. Britvich, V.G. Vasilchenko, I.I. Bushinskaya, E.A. Krivandina, B.P. Sobolev, M. Kobayashi, V.A. Kozlov, M.M. Litvinov, Radiation resistant multicomponent inorganic materials for homogeneous EM calorimeters, Nucl. Instrum. Methods A, 321 (1992) 64-68. https://doi.org/10.1016/0168-9002(92)90378-H.

[15] V.A. Nefedov, “Cherenkov detector” USSR Patent No.1817932 (1991).

[16] A. Mendez-Blas, M. Rico, V. Volkov, C. Zaldo, C. Cascales, Crystal field analysis and emission cross sections of Ho3+ in the locally disordered single-crystal laser hosts M+Bi(XO4)2 (M+=Li,Na; X=W ,Mo), Phys. Rev. B 75 (2007) 174208 1-14. https://doi.org/10.1103/PhysRevB.75.174208.

[17] C. Cascales, C. Zaldo, Comment on “Spectra and energy levels of Er3+ (4f(11)) in NaBi(WO4)2”, J. Appl. Phys., 96 (2004) 4656-4658. https://doi.org/10.1063/1.1792382.

[18] A. Waskowska, L. Gerward, J.S. Olsen, M. Maczka, T. Lis, A. Pietraszko, W. Morgenroth, Low-temperature and high-pressure structural behaviour of NaBi(MoO4)2 - an

X-ray diffraction study. J. Solid State Chem. 178 (2005) 2218–2224. https://doi.org/10.1016/j.jssc.2005.05.001.

[19] L.X. Pang, D. Zhou, Z.M. Qi, Z.X. Yue, Influence of W substitution on crystal structure, phase evolution and microwave dielectric properties of (Na0.5Bi0.5)MoO4 ceramics with low sintering temperature, Sci. Rep. 7 (2017) 3201 1-6. https://doi.org/10.1038/s41598-017-03620-0.

[20] D. Zhou, W.B. Li, H.H. Xi, L.X. Pang, G.S. Pang, Phase composition, crystal structure, infrared reflectivity and microwave dielectric properties of temperature stable composite ceramics (scheelite and zircon-type) in BiVO4–YVO4 system. J. Mater. Chem. C 3 (2015) 2582–2588. https://doi.org/10.1039/C4TC02728K.

[21] J. Hanuza, M. Maczka, J.H. van der Maas, Polarized IR and Raman spectra of tetragonal NaBi(WO4)2, NaBi(MoO4)2 and LiBi(MoO4)2 single crystals with scheelite structure, J. Mol. Struct. 348 (1995) 349-352. https://doi.org/10.1016/0022-2860(95)08660-N.

[22] B.A. Sal, Synthesis and Structural Properties of Nanocomposites Based on Synthetic Opals and Active Dielectrics, Appl. Phys. Res.12 (2020) 19-25. https://doi.org/10.5539/apr.v12n1p19.

[23] J. Hanuza, M. Maczka, L. Macalik, J.H. van der Maas, Polarized Raman spectra of NaBi(MoO4)2 crystal and order-disorder effect in solid scheelites, J. Mol. Struct. 325 (1994) 119-124. https://doi.org/10.1016/0022-2860(94)80026-X.

[24] A.A. Kaminskii, S.N. Bagayev, K. Ueda, H. Nishioka, Y. Kubota, X. Chen, A. Kholov, Efficient stimulated Raman scattering in tetragonal laser crystalline hosts NaBi(MoO4)2 and NaBi(WO4)2, Jpn. J. Appl. Phys. 34 (1995) L1461-L1463. https://doi.org/10.1143/JJAP.34.L1461.

[25] J. Hanuza, M. Maczka, Vibrational properties of the double molybdates MX(MoO4)2 family (M = Li,Na,K,Cs; X = Bi,Cr), Vib. Spectrosc. 7 (1994) 85-96. https://doi.org/10.1016/0924-2031(94)85044-5.

[26] M. Maczka, E.P. Kokanyan, J. Hanuza, Vibrational study and lattice dynamics of disordered NaBi(WO4)2, Raman Spectrosc. 36 (2005) 33–38. https://doi.org/10.1002/jrs.1263.

[27] P. Painter, M. Starsinic, M. Coleman, Determination of functional groups in coal by Fourier transform interferometry, Academic Press: New York, 1985.

[28] S.H. Wang, P.R. Griffiths, Resolution enhancement of diffuse reflectance I.R. spectra of coals by Fourier self-deconvolution: 1. C–H stretching and bending modes, Fuel 64 (1985) 229–236. https://doi.org/10.1016/0016-2361(85)90223-6.

[29] P.R. Solomon, R.M. Carangelo, FTIR analysis of coal. 2. Aliphatic and aromatic hydrogen concentration, Fuel 67 (1988) 949–959. https://doi.org/10.1016/0016-2361(88)90095-6.

[30] A. Gopanna, R.N. Mandapati, S.P. Thomas, K. Rajan, M. Chavali, Fourier transform infrared spectroscopy (FTIR), Raman spectroscopy and wide-angle X-ray scattering (WAXS) of polypropylene (PP)/cyclic olefin copolymer (COC) blends for qualitative and quantitative analysis, Polym. Bull. 76 (2019) 4259-4274. https://doi.org/10.1007/s00289-018-2599-0.

[31] C. Chapa-González , A.L. Pinon-Urbina, P.E. Garcia-Casillas, Synthesis of Controlled-Size Silica Nanoparticles from Sodium Metasilicate and the Effect of the Addition of PEG in the Size Distribution, Materials, 11 (2018) 510 1-7. http://dx.doi.org/10.3390/ma11040510.

[32] P.L. Juchem , T.M.M. de Brum, A.C. Fischer, N.M. Balzaretti, A.H. Augustin, Fuchsite quartzite as an imitation of emerald, J. Gemmol. 30 (2006) No:3/4.

[33] M.L. Johnson, S. Elen, S. Muhlmeister, On the identification of various emerald filling subtances. Gems Gemol. 35 (1999) 82-107. https://doi.org/10.5741/GEMS.35.2.82.

[34] L. Kiefert, H.A. Hanni, J.P. Chalain, W. Weber, Identification of filler substances in emeralds by infrared and Raman spectroscopy. J. Gemmol. 26 (1999) 501-520.

[35] R.H. Bube, Photoelectronic Properties of Semiconductors, Cambridge University Press, 1992.

[36] M. Nagaraja, P. Raghu, H.M. Mahesh, J. Pattar, Structural, optical and Urbach energy properties of ITO/CdS and ITO/ZnO/CdS bi-layer thin films, J. Mater. Sci. Mater. El. 32 (2021) 8976-8982. https://doi.org/10.1007/s10854-021-05568-4.